Mechatronics 19 (2009) 205–217

Contents lists available at ScienceDirect

Mechatronics

journal homepage: www.elsevier.com/locate/mechatronics

Generation of rhythmic and voluntary patterns of mastication using Matsuoka oscillator for a humanoid chewing robot

W.L. Xu [a,*], F. Clara Fang [b], J. Bronlund [a], J. Potgieter [a]

[a] School of Engineering and Technology, Massey University, Albany, Northshore, Auckland, New Zealand
[b] College of Engineering, Technology and Architecture, University of Hartford, Connecticut, USA

ARTICLE INFO

Article history:
Received 8 October 2007
Accepted 19 August 2008

Keywords:
Neural oscillator
Chewing robot
Robotic jaw
Mastication
Muscle activity
CPG

ABSTRACT

We intend to apply Matsuoka neural oscillator into humanoid chewing robots to generate rhythmic actuation of central pattern generator (CPG) and adapt it for voluntary actuation due to sensory feedback. In this paper a single Matsuoka oscillator of two neurons is used for two phase-locked muscles (e.g. masseter and digastric muscles) or for a single robotic joint. To help design and tune the oscillator we have developed three graphical user interfaces (GUI) with aid of which the simulation, parameters' influence and adaptation of the oscillator can be analysed and for specific pattern of muscle activities the oscillator can be selected. Discussions are made in relation to the experimentally confirmed EMG (electromyography) of muscle activities for various foods. A case study involving a jaw, driven by a couple of opening and closing muscles that are commanded by motoneurons is presented. The force of the muscles is described in nonlinear Hill model while the motoneuron for muscle activities is modelled in the oscillator. Simulations are performed to show the oscillator's ability in generating and adapting its rhythmic outputs with respect to the chewing without food (i.e, EMG only for rhythmic muscle activities), with foods (i.e., EMG for rhythmic and additional muscle activities) and with crushable foods (to see how quickly the oscillator to reduce its force commands in order not to damage the teeth). Our work is also meaningful for brain-based control of assistive or rehabilitative devices and EMG-driven neuromusculoskeletal models.

1. Introduction

Human mastication is continually modified throughout the chewing sequence in response to the food dynamics; and mastication patterns vary between subjects and between food textures. This interactive relationship has been utilized to evaluate textural properties of foods by measurement of masticatory psychology [1,2]. The challenge in evaluating foods this way is that full physiologies of mastication can hardly be measured completely and the measurement interferes natural chewing to certain extent. As result, the food texture can only be evaluated qualitatively and various hypotheses could not be tested on human subjects easily.

To this end, a chewing robot solution has been proposed [3,4]. The idea is that while being chewed by a robot, food properties and texture change during chewing are evaluated by robotic states in actuation, chewing force, and/or jaw movements. Although it could be used to chew foods, WJ (Waseda Jaw) robot series was developed to work especially with a WY series dental training robot [5,6]. They did not take into account of the biological aspects of the human masticatory system; and hence the robotic states can not be used for purpose of foods evaluation. The chewing robot [7,8] was based on biomechanical findings about the jaw structure and muscles of mastication, and developed especially for foods evaluation. The above robots may be commanded to chew foods by following recorded masticatory movements and chewing forces, but not mimicking the way human does.

Human chewing of foods is performed by the movement of the jaw that is actuated by the muscles of mastication. Alpha-motoneurons (or alpha-MN) innervate a muscle by recruiting a number of motor units and firing them at various frequencies [9,10]. Electromyography (EMG) measurements have confirmed that a small amount of muscle activities is required for the free rhythmic movements of the jaw, which is produced by central pattern generator (CPG); and additional voluntary muscle activities is generated in alpha-MN if the closing movement is resisted by foods [11,12] and the harder the food, the larger the muscle activities is required [13,14]. In principal, the muscle of mastication involves anticipatory (or feedforward) activities for pre-programmed movement depending on individual chewing expectation, rhythmic activities generated by CPG that is dictated by individual physiology, and voluntary (sensory feedback) activities for overcoming food resistance. To make a chewing robot chew human way, the above mentioned rhythmic, anticipatory, voluntary patterns of muscle activities should be implemented.

* Corresponding author.
E-mail address: W.L.Xu@Massey.ac.nz (W.L. Xu).

0957-4158/$ - see front matter © 2008 Elsevier Ltd. All rights reserved.
doi:10.1016/j.mechatronics.2008.08.003

A CPG can produce coordinated rhythmic muscle activities without any sensory input. It has been modelled as a system of neural oscillators, such as Ellias–Grossberg oscillator [15], Matsuoka oscillator [16], RIO [17], van der Pol oscillator [18]. These CPG models can not only generate robust, sustained oscillation that are necessary for many human body's movements, such as chewing, locomotion, heart beats, breathing, but also be modulated to induce gait transition or variations smoothly [19]. Matsuoka oscillator based CPG model has been popular for humanoid control of robots, such as robot arm and legged robot [20,21], where the dynamics of the robots are exploited to entrain the oscillators.

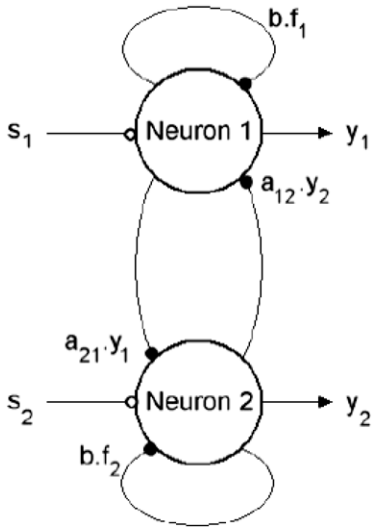

Fig. 1. A Mastuoka oscillator of two neurons.

We intend to apply Matsuoka neural oscillator into humanoid chewing robots to generate rhythmic actuation of CPG and adapt it for voluntary actuation due to sensory feedback. In this paper we present our very first attempt towards the humanoid robotic chewing, where a Matsuoka oscillator of two neurons serves two phase-locked muscles (e.g. masseter and digastric muscles) or a single robotic joint. The hypothesis is that each of the joints (as muscles) of the chewing robot [4,7,8] if actuated using a Matsuoka oscillator would result in the humanoid chewing behaviour of the robot. To help design a neural oscillator, we have developed a design tool, with aid of which the influence of each individual model's parameters on the behaviour (phase, frequency, amplitude) of the oscillator can be analysed and an oscillator can be thus designed for specified behaviours. Measured EMG of muscle activities are generated by the oscillator. A case study involving a jaw, a pair of opening and closing muscles and a motoneuron oscillator is presented. Simulations are conducted to show the oscillator's ability in generating and adapting its rhythmic outputs with respect to various food resistances.

2. Fundamental of Matsuoka oscillator

We consider a simple Matsuoka oscillator to generate/adapt masticatory pattern of two phase-locked muscle activities. The oscillator, as illustrated in Fig. 1, consists of two neurons that are connected in mutually inhibitory fashion. When one neuron (e.g., for the closing muscle of mastication) is activated the other neuron (e.g., for the opening muscle) is suppressed; versa versus. The firing of the neurons is alternated.

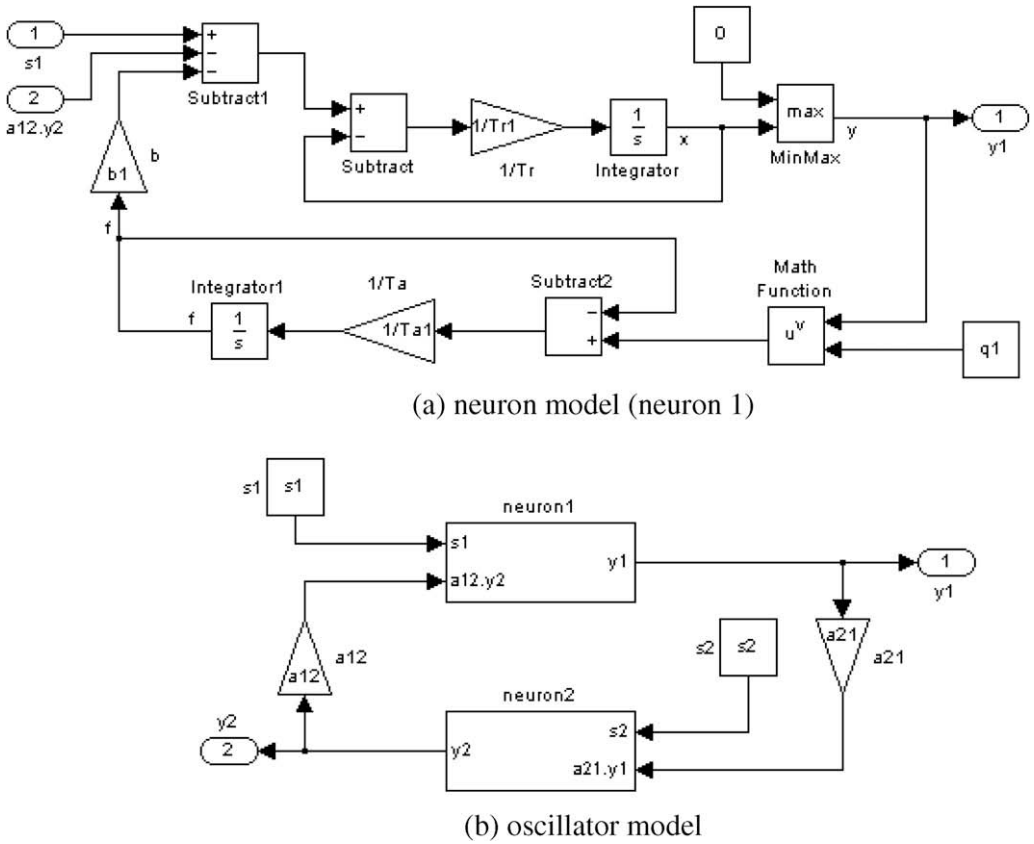

Fig. 2. Matsuoka oscillator in Matlab/Simulink.

The dynamics of the neuron is governed by [16]

$$T_{ri}\frac{dx_i}{dt} + x_i = -a_{ij}y_j + s_i - b_i f_i; \quad (1)$$

$$y_i = g(x_i); \quad (2)$$

$$T_{ai}\frac{df_i}{dt} + f_i = y_i^q; \quad (3)$$

in which $i, j = 1$ or 2 for neuron 1 or 2, x_i is the state of neuron i, s_i the tonic input, y_i the output firing rate, T_{ri} the rise time constant, T_{ai} the adaptation time constant, a_{ij} the weight of inhibitory connection from neuron j to neuron i, f_i represents the degree of fatigue or adaptation in the neuron i, b_i the adaptation firing rate, q_i an exponent for that the adaptation effect is in proportion to a power of the output firing rate, and $g(x)$=max$(x,0)$ is a threshold function.

We put the above oscillator in Matlab/Simulink (Fig. 2) in which each and every oscillator's parameter can be varied. For the oscillator to produce a sustained oscillation, the firing rate constant (b_1 and b_2) must be large and satisfy the criteria provided in [16]. After a short transient period, the two outputs of the oscillator become stable but phase-locked due to the mutual inhibition; and

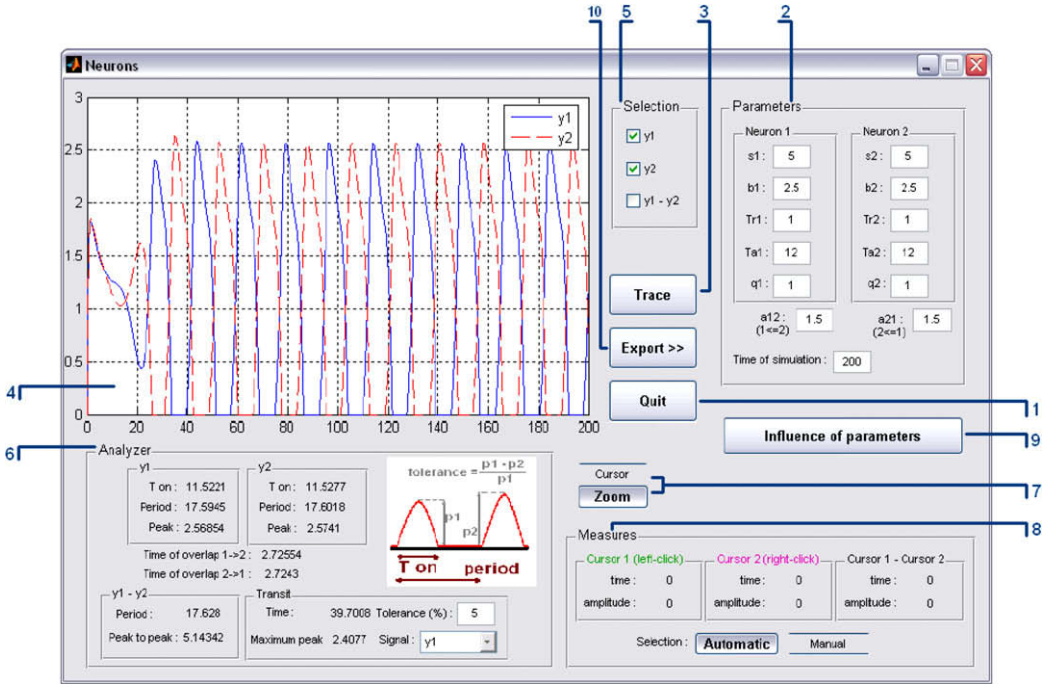

Fig. 3. GUI for simulation.

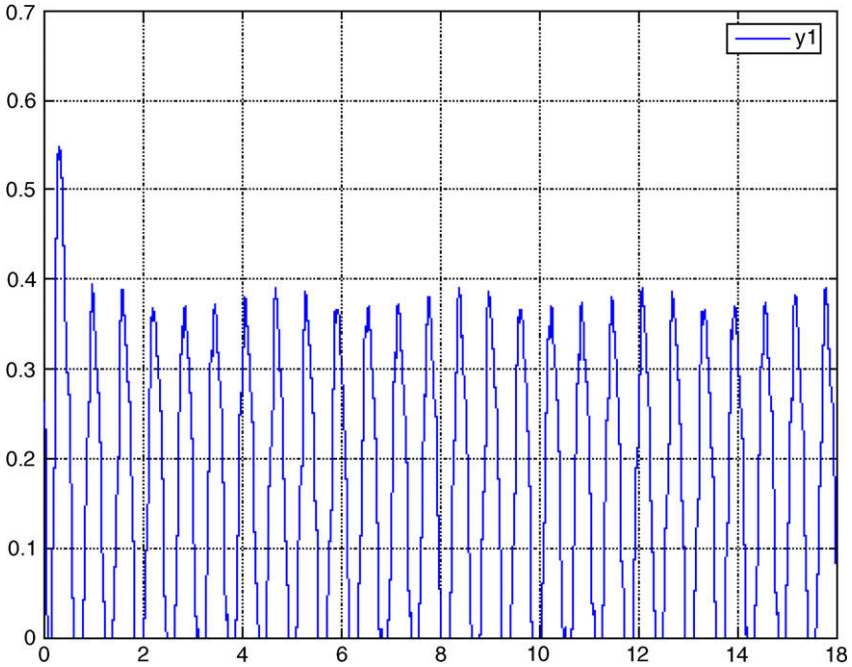

Fig. 4. An EMG muscle activity generated by the oscillator.

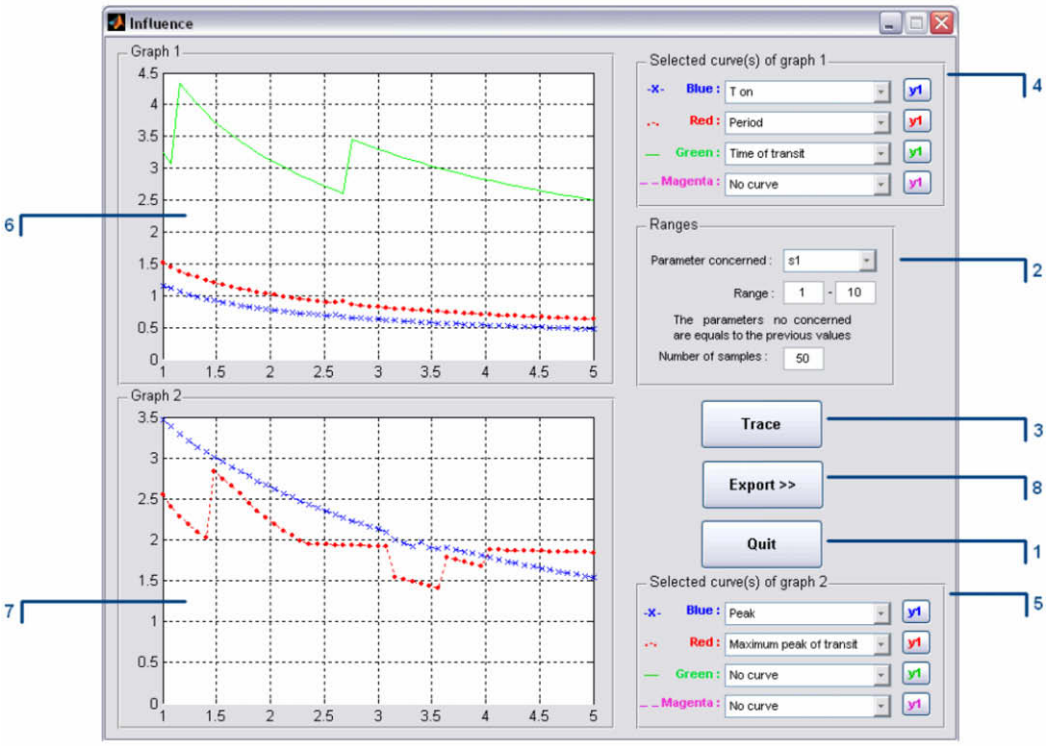

Fig. 5. GUI for influence analysis.

their alternating firing results from the adaptation in the currently firing neuron and the building-up of the activity in the other neuron. It was found that the frequency of the oscillation is positively correlated to the firing rate constant, and negatively correlated to the rise time constant, adaptation time constant and connection weights, while the amplitude of the oscillation is directly proportional to the increment of the tonic input [22].

3. Tuning of Mastuoka oscillator for rhythmic and voluntary muscle activities

The oscillator (Fig. 1) may be used to produce up to three rhythmic outputs, i.e., y_1, y_2 and $y_1 - y_2$. For example, for a pair of jaw closing and opening muscles, two phase-locked outputs y_1 and y_2 are required for the motoneuronal control; and for a joint of a robotic arm, the output $y_1 - y_2$ is necessary for motion commands [20]. An output of the oscillator consists of both transient and sustained oscillation and consequently, it may be characterized by a number of measurements, such as frequency, amplitude, phase overlapping (of y_1, y_2), transient time and transient peak etc, depending on its application. As the oscillator involves a number of parameters and various measurements, for which there also are no simple analytical closed-form relationships available, to help tune the oscillator for prescribed behaviours of oscillation, we have developed three user interfaces (GUIs) in Matlab based on the model shown in Fig. 2. The GUIs are more easily comprehended than other design methods, such as describing function [20] and numerical method [22]. The first GUI (Fig. 3) is useful for simulating the behaviour of the designed oscillator, the second GUI (Fig. 5) is helpful in selecting the values of the oscillator's

Table 1
Influence analysis, $q = 1$

	Ton		Period		Peak		Time of transit		Max peak of transit		Time of overlap	
	y_1	y_2	y_1	y_2	y_1	y_2	y_1	y_2	y_1	y_2	$y_1 \Rightarrow y_2$	$y_2 \Rightarrow y_1$
s_1	↑	↓	≈	≈	↑	↔	↓	↑	↑	↔	↓	↑
s_2	↓	↑	≈	≈	↔	↑	↑	↓	↔	↑	↑	↓
s_1 and s_2	↔	↔	↔	↔	↑	↑	↔	↔	↑	↑	↔	↔
b_1	↓	↔	↓	↓	↓	↓	↓	↓	↓	↔	↑	↓
b_2	↔	↓	↓	↓	↓	↓	↓	↓	↔	↓	↓	↑
b_1 and b_2	↓	↓	↓	↓	↓	↓	↓	↓	↓	↓	↓	
T_{r1}	↑	↑	↑	↑	↓	↔	↑	↑	↔	↔	↑	↑
T_{r2}	↑	↑	↑	↑	↔	↓	↑	↑	↔	↔	↑	↑
T_{r1} and T_{r2}	↑	↑	↑	↑	↓	↓	↑	↑	↔	↔	↑	↑
T_{a1}	↑	↑	↑	↑	↔	↔	↔	↑	≈	≈	↑	↑
T_{a2}	↑	↑	↑	↑	↔	↔	↑	↔	≈	≈	↑	↑
T_{a1} and T_{a2}	↑	↑	↑	↑	↔	↔	↑	↑	≈	≈	↑	↑
a_{12}	≈	↑	↑	↑	↑	↔	↑	↑	≈	≈	≈	↓
a_{21}	↑	≈	↑	↑	↔	↑	↑	↑	≈	≈	↓	≈
a_{12} and a_{21}	↑	↑	↑	↑	↑	↑	↑	↑	≈	≈	↓	↓

Table 2
Influence analysis, $q > 1$

	Ton		Period		Peak		Time of transit		Max peak of transit		Time of overlap	
	y_1	y_2	y_1	y_2	y_1	y_2	y_1	y_2	y_1	y_2	$y_1 \Rightarrow y_2$	$y_2 \Rightarrow y_1$
s_1	↑	↓	↓	↓	↑	↔	≈	≈	↑	↔	↓	↑
s_2	↓	↑	↓	↓	↔	↑	≈	≈	↔	↑	↑	↓
s_1 and s_2	↓	↓	↓	↓	↑	↑	↓	↓	↑	↑	↓	↓
b_1	↓	↔	↓	↓	↓	↓	≈	≈	↓	↔	↑	↓
b_2	↔	↓	↓	↓	↓	↓	≈	≈	↔	↓	↓	↑
b_1 and b_2	↓	↓	↓	↓	↓	↓	↓	↓	↓	↓	↓	↓
T_{r1}	↑	↑	↑	↑	↓	↔	↑	↑	↔	↔	↑	↑
T_{r2}	↑	↑	↑	↑	↔	↓	↑	↑	↔	↔	↑	↑
T_{r1} and T_{r2}	↑	↑	↑	↑	↓	↓	↑	↑	↔	↔	↑	↑
T_{a1}	↑	↑	↑	↑	↔	↔	↔	↑	≈	≈	↑	↑
T_{a2}	↑	↑	↑	↑	↔	↔	↑	↔	≈	≈	↑	↑
T_{a1} and T_{a2}	↑	↑	↑	↑	↔	↔	↑	↑	≈	≈	↑	↑
a_{12}	≈	↑	↑	↑	↑	↔	≈	≈	≈	≈	≈	↓
a_{21}	↑	≈	↑	↑	↔	↑	≈	≈	≈	≈	↓	≈
a_{12} and a_{21}	↑	↑	↑	↑	↑	↑	≈	≈	≈	≈	↓	↓

Table 3
Influence analysis, $q < 1$

	Ton		Period		Peak		Time of transit		Max peak of transit		Time of overlap	
	y_1	y_2	y_1	y_2	y_1	y_2	y_1	y_2	y_1	y_2	$y_1 \Rightarrow y_2$	$y_2 \Rightarrow y_1$
s_1	↑	↓	≈	≈	↑	↑	≈	≈	↑	↔	↓	↑
s_2	↓	↑	≈	≈	↑	↑	≈	≈	↔	↑	↑	↓
s_1 and s_2	↑	↑	↑	↑	↑	↑	↑	↑	↑	↑	↑	↑
b_1	↓	↔	↓	↓	↓	↓	≈	≈	↓	↔	↑	↓
b_2	↔	↓	↓	↓	↓	↓	≈	≈	↔	↓	↓	↑
b_1 and b_2	↓	↓	↓	↓	↓	↓	↓	↓	↓	↓	↓	↓
T_{r1}	↑	↑	↑	↑	↓	↔	↑	↑	↔	↔	↑	↑
T_{r2}	↑	↑	↑	↑	↔	↓	↑	↑	↔	↔	↑	↑
T_{r1} and T_{r2}	↑	↑	↑	↑	↓	↓	↑	↑	↔	↔	↑	↑
T_{a1}	↑	↑	↑	↑	↔	↔	↔	↑	≈	≈	↑	↑
T_{a2}	↑	↑	↑	↑	↔	↔	↑	↔	≈	≈	↑	↑
T_{a1} and T_{a2}	↑	↑	↑	↑	↔	↔	↑	↑	≈	≈	↑	↑
a_{12}	≈	↑	↑	↑	↑	↔	↑	↔	≈	≈	≈	≈
a_{21}	↑	≈	↑	↑	↔	↑	≈	↑	≈	≈	≈	≈
a_{12} and a_{21}	↑	↑	↑	↑	↑	↑	↑	↑	≈	≈	≈	≈

parameters to achieve the specified behaviours, and the third GUI (Fig. 6) is to visualise or predict adaptive behaviour of the oscillator with varying parameters.

3.1. GUI for simulation of the oscillator

The first GUI (Fig. 3) is for simulation of the oscillator with known value of the parameters. The values of the oscillator's parameters are supplied directly by typing into spaces (labelled 2) located at the upper right corner of the GUI. Single or multiple outputs of y_1, y_2 and $y_1 - y_2$ can be selected (5), traced (3) and displayed in the window (4). The measurements, including Period for the frequency, T_{on} for the duty cycle, Peak for the amplitude of the oscillation, Time of Overlapping (of y_1 and y_2) and Transient Time and Maximum Peak can be displayed automatically (6) or measured manually using a combination of cursor and mouse click (8). The radio button Export $\gg$ (10) is for separate production of the output diagrams (e.g., Figs. 4 and 6).

The default example seen in the GUI was taken from Masuoka [16]. The sustained oscillations of y_1 and y_2 match those in the reference, but involve also a transient of around 20 s that is roughly one cycle of the sustained oscillation. This transient dynamics is appreciated in engineering applications of Matsuoka oscillator.

An EMG muscle activity of the right masseter muscle measured while a subject was chewing on almond [13] is reproduced, as shown in Fig. 4. The oscillator (that was found via GUI shown in Fig. 5, to be discussed below) has the following parameters, $s_1 = s_2 = 1$, $b_1 = b_2 = 2.5$, $T_{r1} = T_{r1} = 0.03$, $T_{a1} = T_{a2} = 0.4$, $q_1 = q_2 = 0.7$, $a_{12} = a_{21} = 1.5$. The major properties of the EMG pattern reproduced are T_{on} = 0.456 s, Period = 0.618 s, Amplitude = 0.380 and Transient Time = 0.78 s, approximately. The generated EMG agrees with the measured one EMG in its most characteristics (e.g., frequency, duty cycle and amplitude).

3.2. GUI for influence analysis of the oscillator parameters

Matsuoka drew partial and qualitative conclusion on the influence of the parameters on the oscillator behaviour, as stated early [16,22]. This is very valuable, but not easy for use of selecting the oscillator to generate the oscillation(s) specific to applications. A GUI (Fig. 5) for this purpose has been developed, by means of which the influence of any oscillator's parameter on any particular feature of the oscillator's behaviour can be analysed. This GUI is embedded in the first GUI and accessed via the button Influence of parameters (9) in Fig. 3. A Matlab program runs behind scene to simulate the oscillator under concern and measure its characteristics.

In the GUI there are two windows Graph 1 and Graph 2 (labelled 6 and 7) to display up to 8 features of the oscillator, each for 4 features selected via the spaces provided at 4 and 5. The features available include duty cycle, period, amplitude, phase overlapping time, transient time and transient amplitude. Any of y_1,

y_2 or $y_1 - y_2$ can be chosen as the output to be analysed (4), but the influence analysis can be performed for only one oscillator parameter at a time. The parameter and its range are set in the left middle area Ranger (2) of the GUI. Pressing the button Trace (3) displays the variations of selected feature versus selected parameter in Graph 1 and Graph 2 windows, and pressing Export ≫ (8) creates more nicely looking graphs in separate sheets, one graph per sheet.

Using this GUI a thorough influence analysis was performed. Tables 1–3 give the results with respect to $q = q_1 = q_2 = 1$, >1 and <1, respectively. Symbol ↑, ↓, ↔, and ≈ there stand for a measure's increment, decrement, no-change and no-tendency with respect to the increment in value of an oscillator's parameter, respectively.

It is interesting to remark the effect of the exponent constant $q = q_1 = q_2$. When $q = 1$, varying s_1 and s_2 varies the amplitude of the oscillation; varying T_{r1}, T_{r2}, T_{a1} and T_{a2} changes frequency (or period) and duty cycle of the oscillation; varying b_1, b_2, a_{12}, and a_{21} changes the shape of the oscillation; and when $q < 1$ or >1, change in s_1 and s_2 changes the amplitude, period and overlapping time simultaneously. A meaningful hint is that when both amplitude and period need to be varied, both s_1 and s_2 may be varied with q being non-unity.

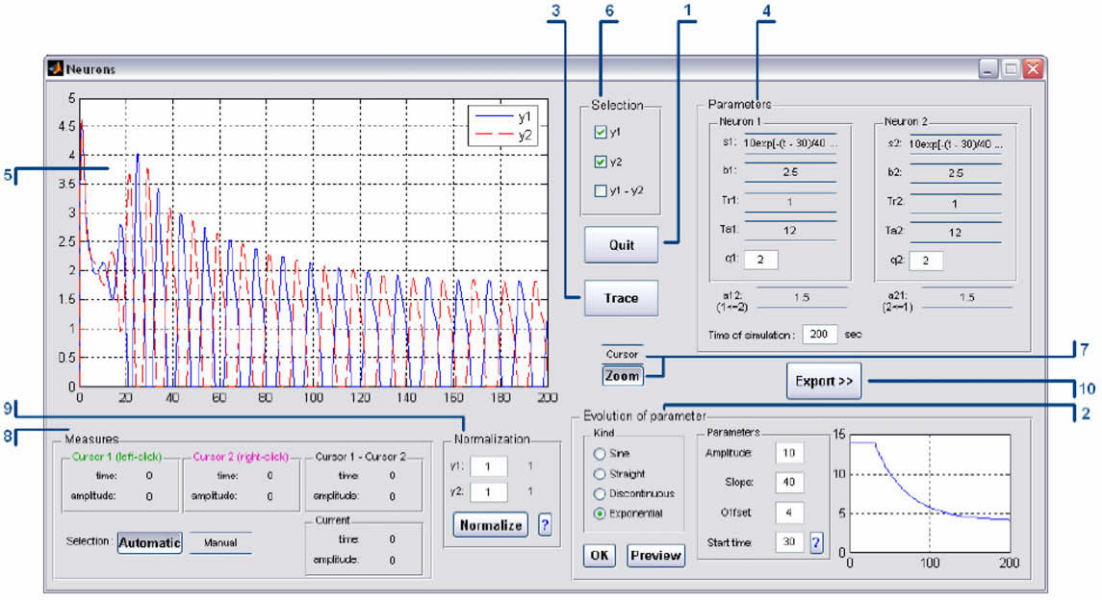

Fig. 6. GUI for adaptation analysis.

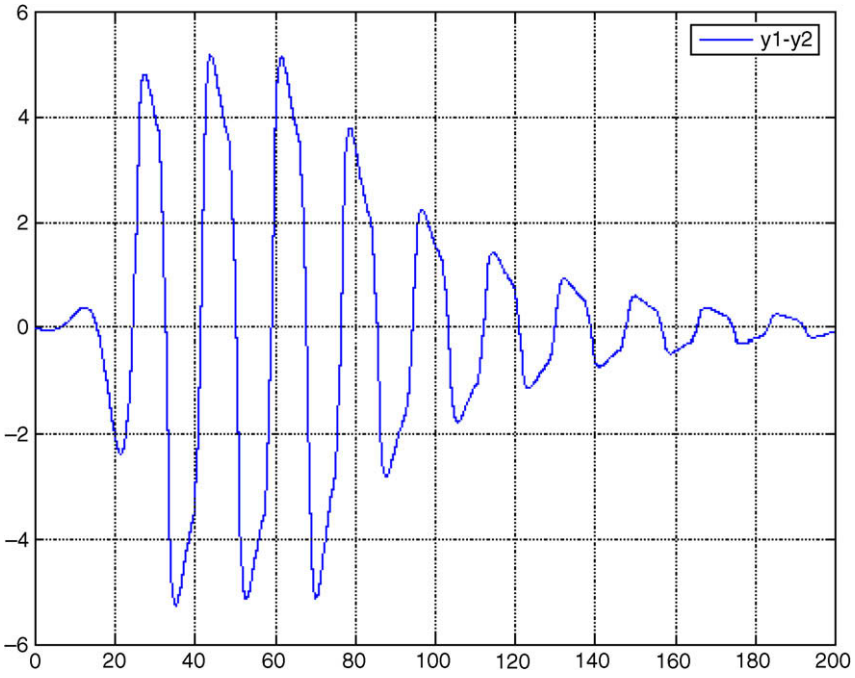

Fig. 7. Output $y_1 - y_2$ for $s_1 = s_2 = 10\exp[-(t - 70)/40]$.

3.3. GUI for adaptation of the oscillator

In applications like modelling human mastication, an oscillator can be used as CPG to generate rhythmic pattern of muscle activity. This requires fixing a value for each parameter of the oscillator. Considerable amount of experiments have confirmed that the rhythmic pattern is invariant for free jaw movements without foods; while chewing on foods, it adapts by the motoneuron quickly in response to the change in food resistance during the chewing process [11–13]. That is to say, if a single oscillator is used to generate central pattern of muscle activity, one or a few of the oscillator parameters need to be adapted in real time in order to have varying voluntary muscle activities required. To simulate how the oscillator behaves over time with respect to varying parameter, a third GUI has been developed, as shown in Fig. 6.

Any of the oscillator parameters can be selected to vary over time. When this is done, the rest of the parameters remain unchanged. The varying parameter is set at Parameters (4) of the GUI and its variation is defined at Evolution of parameter (2). There are four options to choose from: Sine (for sinusoid function), Straight (for constant or linear function), Discontinuous (for any discrete function specified in data sets) and Exponential (for exponential function). Once a function is chosen and specified, it can be previewed, and if satisfactory, then confirmed.

The chosen output of the oscillator is displayed in the window (5). The output can be normalised to any range using the spaces

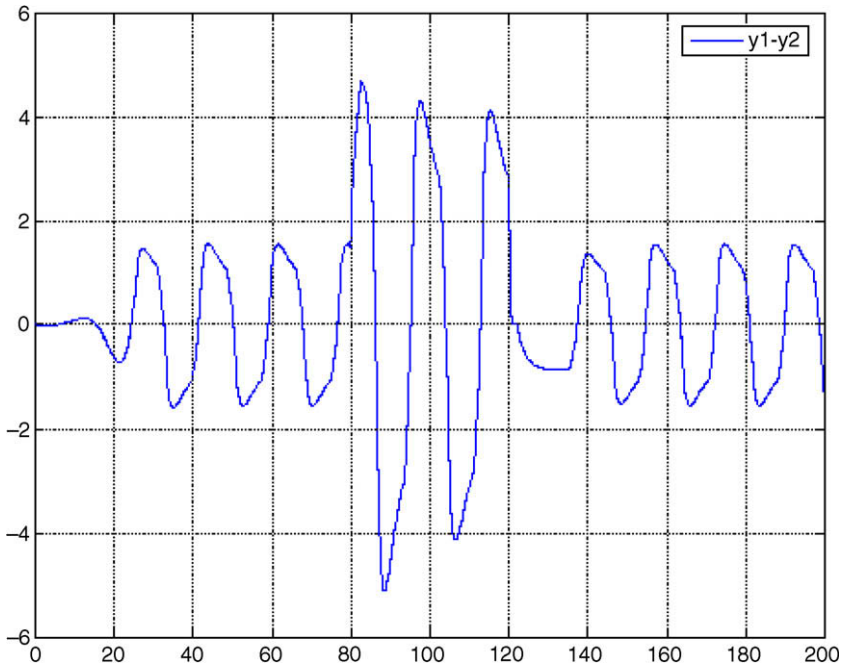

Fig. 8. Output $y_1 - y_2$ for $s_1 = s_2 = 3$ for 0–80 s, 8 for 80–120 s and 3 for 120–200 s.

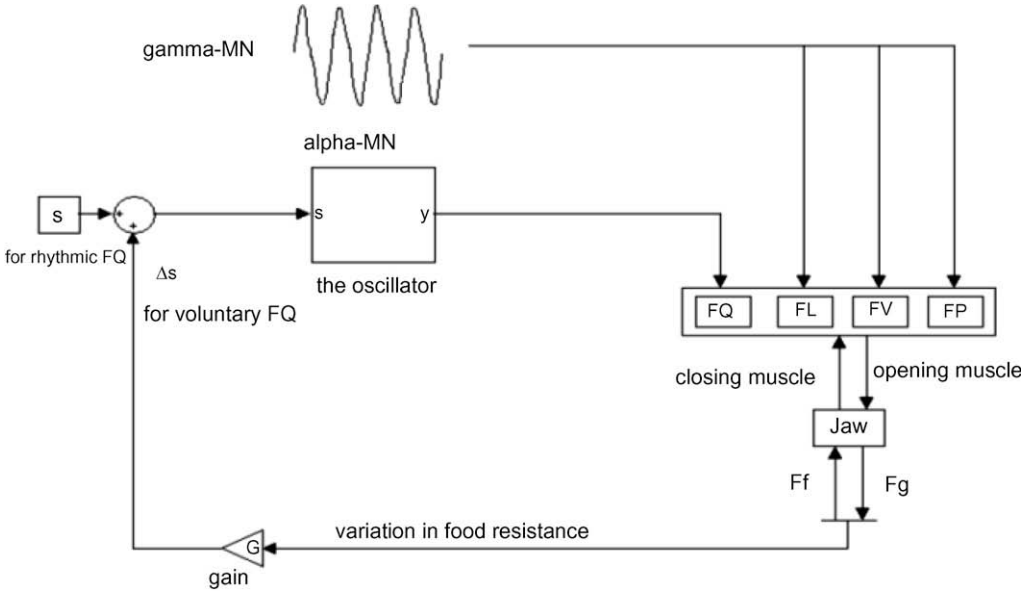

Fig. 9. Rhythmic and voluntary muscle activities in a simplified jaw system.

at Normalisation (9). The rest of the GUI features are similar to the other GUIs. The output can also be measured at any time point by cursor and mouse click (8).

The default example in the GUI (Fig. 6) is for exponential variation of s_1 and s_2 with $q_1 = q_2 = 2$ and Fig. 7 shows another output $y_1 - y_2$ for $s_1 = s_2 = 10e^{-(t-70)/40}$ and $q_1 = q_2 = 2$. It can be seen from both examples that the oscillator output y_1, y_2 and $y_1 - y_2$ have a decreasing amplitude and increasing period over time. For another example (Fig. 8), $s_1 = s_2$ is set 8 for the period of 80–120 s and 3 for the rest of the time. The result has confirmed the oscillator adapts its behaviour very quickly and changes its stable oscillation from one to another within a cycle. In this example, the oscillation adapts its amplitude at 80 s and 120 s without much transient.

4. Case study in rhythmic and voluntary mastication

4.1. The purpose of and assumption for the case study

The jaw is actuated alternatively by a group of opening and closing muscles, resulting in rhythmic chewing movements. The masticatory system is a typical neuromotor system whose simplest functional unit is a motor unit consisting of an alpha-motoneuron and the muscle fibres it innervates [9]. To increase muscle force, the central nervous system may recruit new motor units and/or increase the frequency of firing of already recruited motor units. For non-clinical applications, muscle activity may be recorded by surface EMG. A reproduced EMG envelope of the masseter activity profiled by filtering, rectification and integration has been illustrated in Fig. 4.

In neuroscience there are two hypotheses about voluntary control of a single muscle [9]. This case study is to apply Mastuoka's oscillator to simulating the so-called servo hypothesis. According to the hypothesis, a voluntary movement of muscle is generated in terms of control using information about the neurophysiological mechanisms of muscle reflexes. CPG, via gamma-MN, sets a value of muscle lengthen, and alpha-MN get the set muscle lengthen served by varying their activities to balance the variation in external load (e.g. food resistance for masticatory muscles). This hypothesis is criticised for large gain in the tonic stretch reflex, but is still attractive in terms of the engineering possibility of its servo control.

Table 4
Muscle parameters for nonlinear Hill model (extracted from [24,25])

Muscle		Initial muscle length Lm (mm)	Initial fibre length Lf (mm)	Initial sarcomere length Ls (μm)	Force max F_{max} (N)
Masseter	Superficial part	45.6 ± 4.2	24.6 ± 4.1	2.47 ± 0.27	272.8
	Deep part	25.3 ± 3.9	18.0 ± 2.8	2.44 ± 0.22	139.6
Temporalis	Anterior part	49.7 ± 3.9	27.1 ± 3.8	2.35 ± 0.14	308
	Posterior part	52.2 ± 4.7	25.7 ± 3.3	2.31 ± 0.12	222
Medial pterygoid	Anterior part	37.9 ± 6.0	13.5 ± 1.9	2.48 ± 0.36	240
	Posterior part	44.4 ± 5.5	12.4 ± 1.5	2.54 ± 0.38	
Lateral pterygoid	Inferior head	32.6 ± 3.1	23.0 ± 2.7	2.83 ± 0.10	112.8
	Superior head	31.3 ± 2.9	21.4 ± 2.2	2.72 ± 0.11	38
Digastric	Posterior belly	54.9 ± 5.5	20.5 ± 2.6	2.72 ± 0.14	Unknown
	Anterior belly	43.2 ± 4.9	21.4 ± 4.5	2.75 ± 0.21	46.4
Geniohyoid		40.0 ± 5.5	34.3 ± 5.1	2.65 ± 0.33	38.8
Mylohyoid	Posterior part	42.6 ± 5.3	28.2 ± 3.3	2.89 ± 0.19	21.2
	Anterior part	23.0 ± 2.8		2.80 ± 0.15	63.6

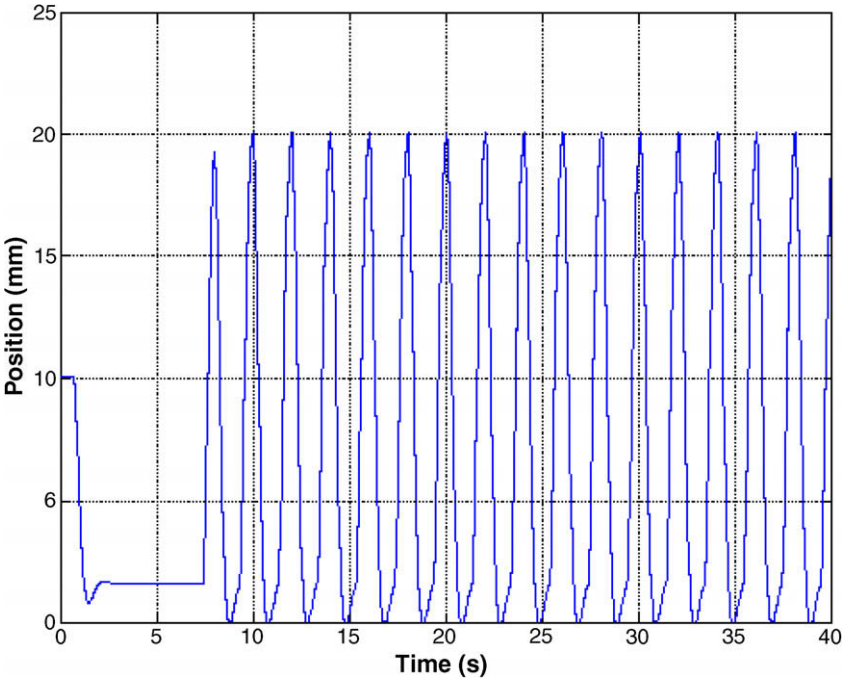

Fig. 10. Jaw movement without food.

This case study assumes that the jaw be driven by a closing muscle (masseter) and an opening muscle (digastric), gamma-MN set the rhythmic muscle activities (for rhythmic jaw movement), and alpha-MN, modelled by the oscillator, generate the voluntary muscle activities. Two outputs, y_1 and y_2 of the oscillator are for alpha-MN activity of the closing and opening muscles, respectively. The oscillator is adapted by the variation in food resistance (F_f) through the two identical tonic inputs s_1 and s_2. Fig. 9 illustrates the case study problem.

4.2. The modelling of the masticatory muscles

Both masseter and digastric muscles are represented by nonlinear Hill model and the force of the muscle is calculated by [23]

$$F = F_{max}(FL \times FV \times FQ + FP) \quad (4)$$

in which F_{max} is the maximum force of a muscle; *FL*, *FV* and *FQ* are force/length factor, force/velocity factor and activation factor, respectively; and *FP* is force scaling factor for the parallel elastic

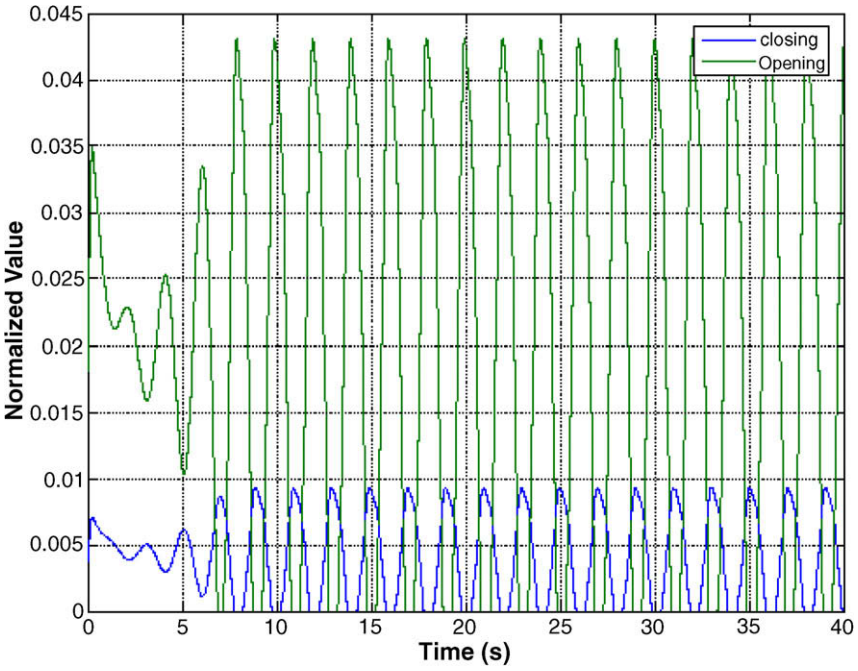

Fig. 11. Normalised FQs without food resistance.

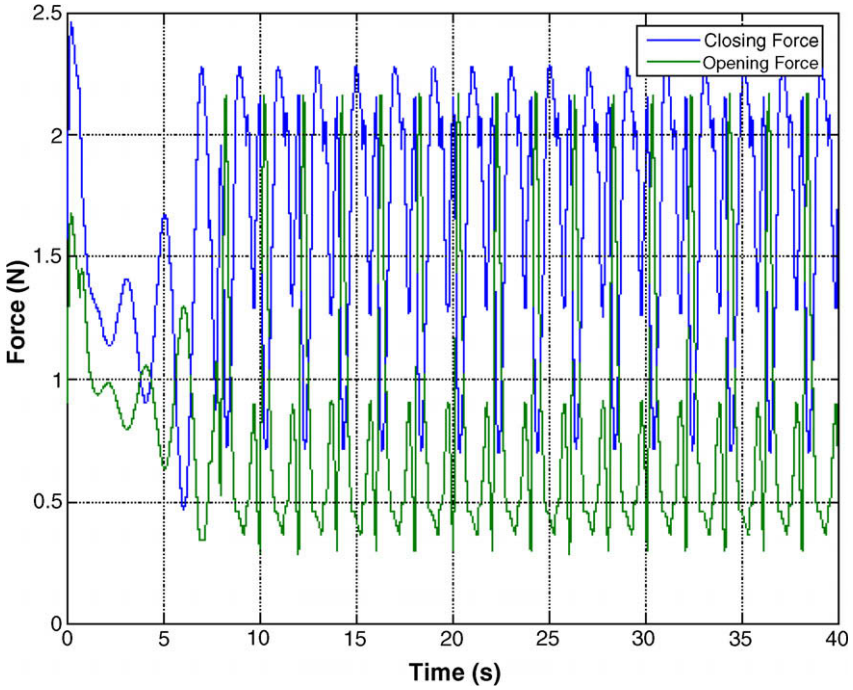

Fig. 12. Muscle forces applied on the jaw without food resistance.

element. It is noted that *FL*,*FV* and *FQ* contribute to the active part of the muscle force and *FP* to the passive part of the muscle force.

While *FQ* depends on the activity in alpha-MN, which is generated by the oscillator or supplied by measured EMG; *FL*, *FV* and *FP* are calculated using instantaneous sarcomere length (or given by gamma-MN activity) of the muscle fibres [23]

$$FL = 0.4128Ls(t)^3 - 4.3957Ls(t)^2 + 14.8003Ls(t) - 15.0515 \quad (5)$$

$$FV = \frac{12.5 - [Vs(t)/2.73]}{12.5 + [Vs(t)/0.49]} \quad \text{for } Vs(t) \geqslant 0;$$

$$1.5 - 0.5\frac{12.5 + [Vs(t)/2.73]}{12.5 - 2[Vs(t)/0.49]} \quad \text{for } Vs(t) < 0 \quad (6)$$

$$FP = 0.0014\exp[6(Ls(t) - 2.73)/2.73] \quad (7)$$

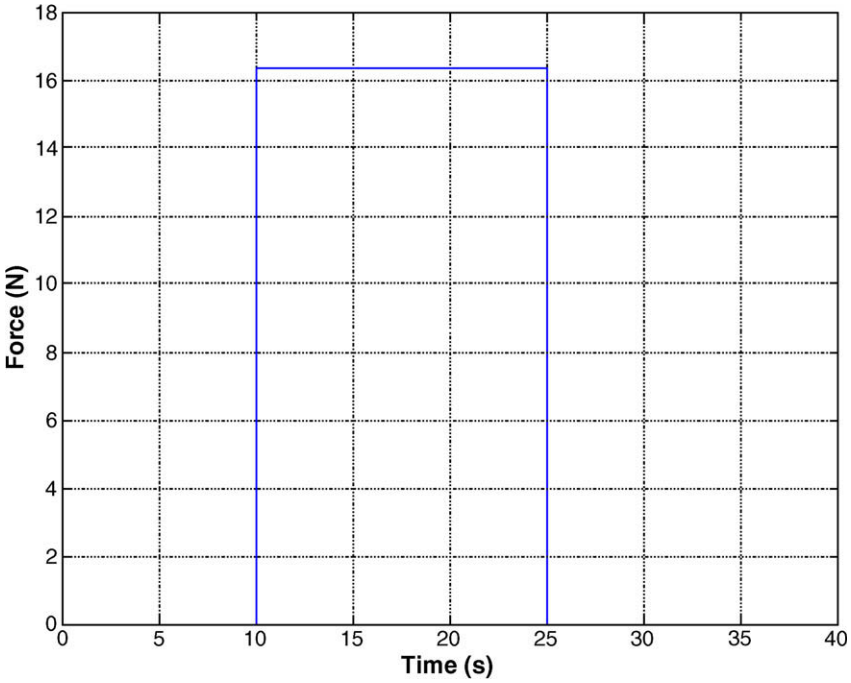

Fig. 13. A step food resistance.

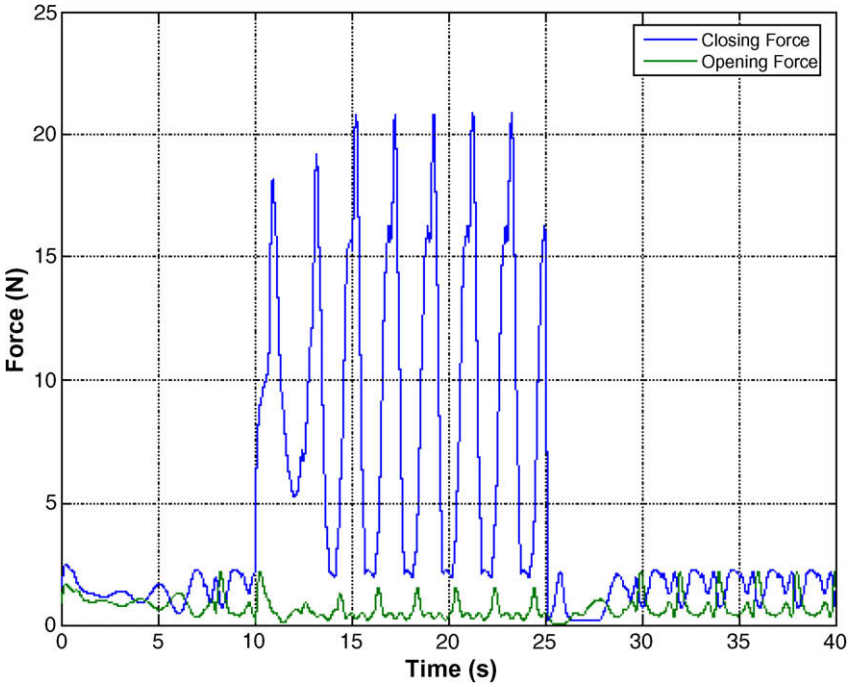

Fig. 14. Muscle forces at a step food resistance.

in which $Ls(t)$ and $Vs(t)$ are the instantaneous length and shorting velocity of the sarcomere, respectively. They can be found by [23]

$$Ls(t) = [Lm(t) - (Lm_i - Lf_i)]\frac{Ls_i}{Lf_1} \tag{8}$$

where Lm_i, Lf_i and Ls_i are the initial muscle length, muscle fibre length and sarcomere length, respectively, whose values are given in Table 4, and the instantaneous muscle length $Lm(t)$ can be scaled from the jaw movement as below.

For the masseter

$$Lm(t) = \frac{0.21Lm_{max}D}{D_{max}} + 0.79Lm_{max} \tag{9}$$

in which Lm_{max}, D and D_{max} are the masseter length when the jaw is fully opened, instantaneous opening of the jaw, and maximum opening of the jaw, respectively. At the full open position the sarcomeres of the masseter are supposed to stretch to 4.0 μm, and then using Eq. (8) Lm_{max} can be found.

For the digastric

$$Lm(t) = \frac{-0.26Lm_{max}D}{D_{max}} + Lm_{max} \tag{10}$$

in which Lm_{max} is the digastric length when the jaw is fully closed. Suppose the digastric sarcomere be decreased to 2 μm at the full close position of the jaw, Lm_{max} for the digastric can be found by Eq. (8).

4.3. Simulations

In the simulation the jaw displaces with amplitude of 20 mm and frequency of 2 Hz; the jaw mass is set 230 g; F_{max} for the masseter is 272.8 N; F_{max} for the digastric is 46.4 N; the masseter (closing muscle) contracts about 20% of its length when jaw is fully closed; and the digastric (opening muscle) contracts about 26% of its lengthen when jaw is fully opened.

The first experiment does not involve any food (or nil food resistance), the alpha-MN oscillator needs to generate a pattern for FQ so that the specified jaw movement is satisfied. The oscillator tuned using the GUIs has the following parameters: $s_1 = s_2 = 5$, $b_1 = b_2 = 2$, $q_1 = q_2 = 1$, $a_{12} = a_{21} = 1.2$, $T_{r1} = 0.06$, $T_{a1} = 0.7$, $T_{r2} = 0.06$, and $T_{a2} = 0.7$. The feedback gain for adjustment in the tonic input $G = 2.17$. Figs. 10–12 show the jaw movement, masseter and digastric FQs and masseter and digastric forces acting on the jaw, respectively.

It can be found from the results that there exists a transient phase in the beginning as the jaw stands still initially; digastric FQ is relatively larger (meaning more activities are required) than masseter's because the digastric is weaker; and a maximum muscle force of 2.5 N is due to a combination of the gravitational, inertia, masseter and digastric forces acting on the jaw. It is worth noting that instantaneous masseter and digastric forces are coupled; and while closing the digastric drags the masseter and while opening the masseter pulls the digastric.

When a constant food force is suddenly added at 10 s and removed at 25 s (Fig. 13), the alpha-MN (or oscillator) reacts immediately and adapts the closing muscle force within a cycle of chewing; and the muscle takes one or two cycles to get to the stable force required to chew the food or get back to the lower force for free rhythmic chewing, as shown in Fig. 14. Due to the inertia and nonlinear behaviours of the muscles, the jaw movement is disturbed at the times the force is applied and removed (Fig. 15). These simulation results are in good agreement of the experimental results that the closing muscles adapt their force within a chewing cycle when the food is suddenly put into or removed from the mouth [13,14]. It is noted that the digastric force does not vary very much during the change in the food resistance.

While being chewed certain foods behave with a gradually decreasing resistance. This scenario is simulated using a force profile (Fig. 16) where at the time 10 s, a food is inserted suddenly and then gradually reduced to nil at 25 s. Fig. 17 shows clearly that the alpha-MN (or oscillator) reacts immediately and adapts the closing muscle force in direct proportion to the food resistance.

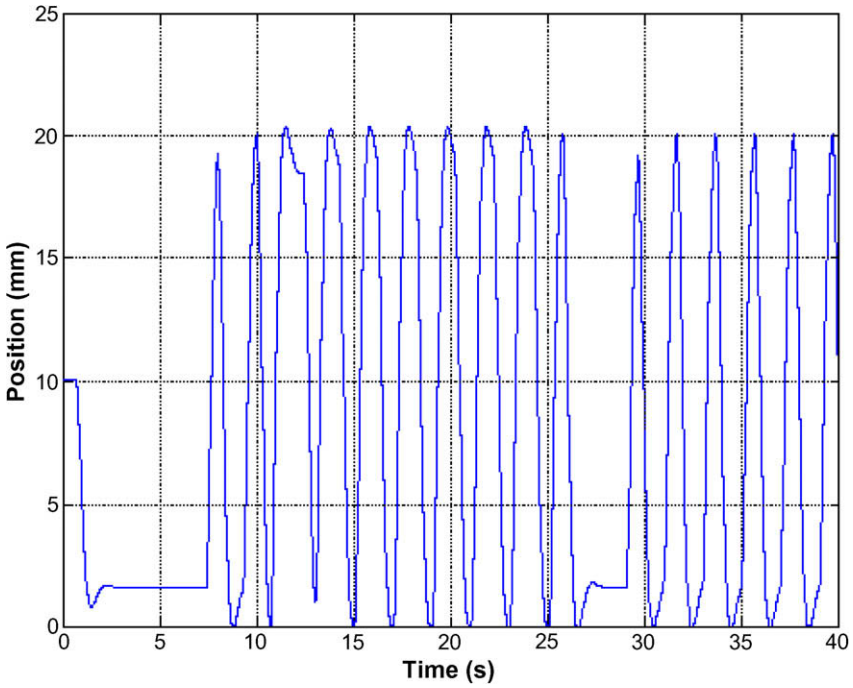

Fig. 15. Jaw movement at a step food resistance.

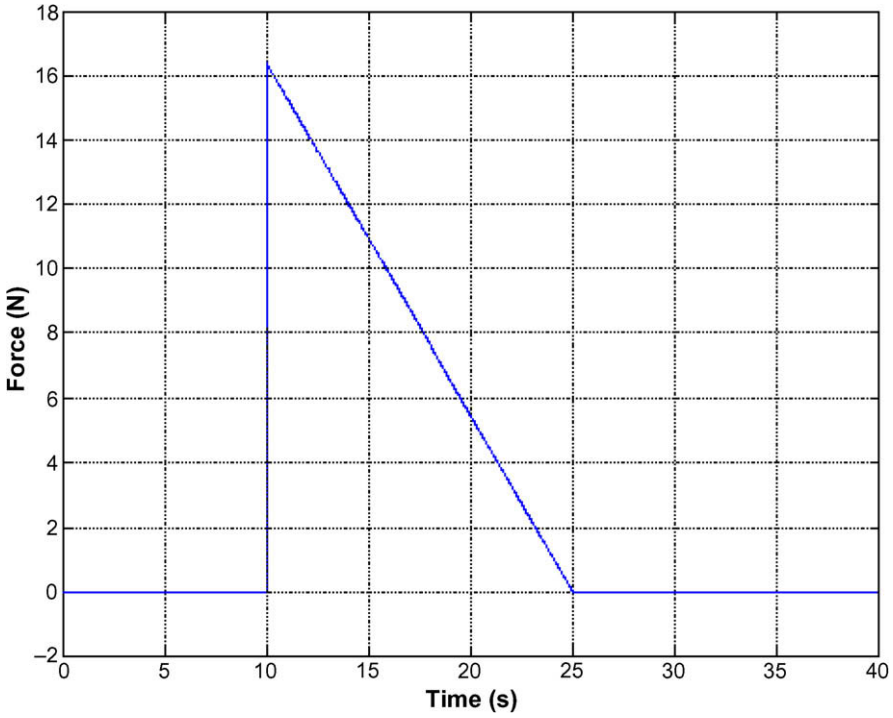

Fig. 16. A force profile simulating the decreasing food resistance.

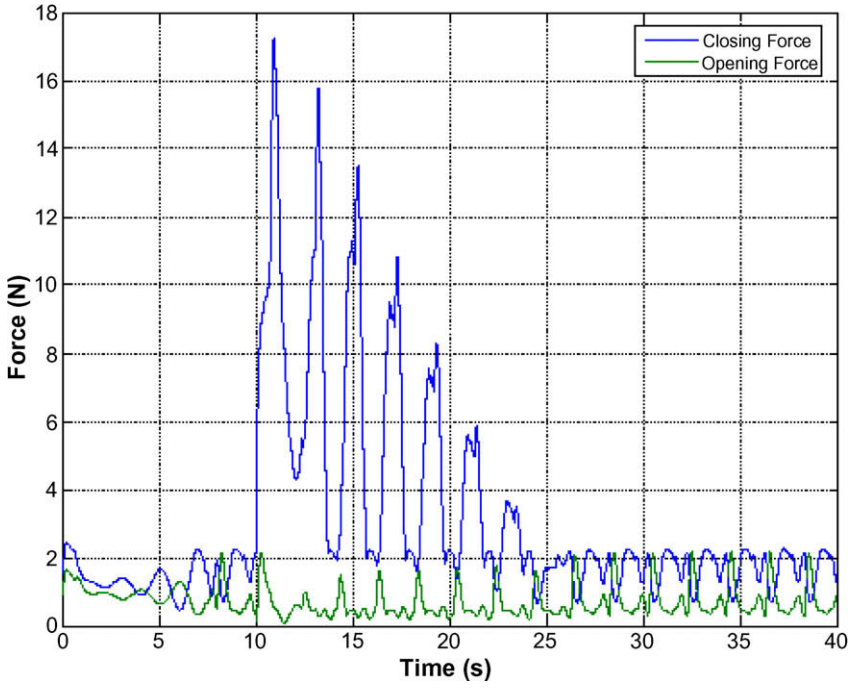

Fig. 17. Muscle force in response to the decreasing food resistance.

It should be noted that the chewing force (or to be exact, occlusal force) changes from cycle to cycle. The magnitude of the force peak of a cycle decreases as the chewing goes on. The force profile within one occlusal phase of a cycle is definitely nonlinear, subject to lots of factors involving foods, jaw/teeth movement and jaw muscle activities. The force profile (Fig. 16) that illustrates the decrement of the peak forces in magnitude is used to test the quick response and adaptation of the Matsuoka oscillator. Figs. 13 and 16 do not mean the actual occlusal force.

5. Conclusion

The Matsuoka oscillator was used to generate rhythmic (CPG) and voluntary (sensory feedback) patterns of muscle activities and intended as a motion generation and its sensory adjustment for humanoid chewing robots. An assistive tool (GUIs) was developed to help analyse and design the oscillator. A full picture of the parameters' influence on various measurement of the oscillation was presented. The use of the oscillator was demonstrated in conjunction with a simplified neuromotor system of the jaw;

and the simulations were performed to validate the capacity of the oscillator in terms of generating additional voluntary muscle activities for various food resistances. The fit of the oscillator as motion commands into our chewing robots is a research objective identified for the aim of humanoid or bionic chewing.

A remark for the real implementation is in order. As mentioned early, the paper presents our very first attempt towards the humanoid robotic chewing using Matsuoka oscillator to command/actuate the robotic joint. While the potential was shown, our current effort has continued on a robotic experimental setup in the manner of hardware-in-loop simulation [26]. In our system the software packages (Matlab, Simulink, RealTime Workshop and xPC Target) are interfaced to a Sensory I/O Board that is followed by a Galil power amplifier to drive a DC motor [8]. The xPC Target provides a rapid prototyping host target environment to construct the real time control system using Matsuoka oscillator.

Acknowledgement

C. Nicolotte of INSA, France, P. Cambonie of INSA, France and P. of ENSIL, Lomoges, France conducted most of the simulations presented in the paper during their research stay at Massey University, Auckland, New Zealand in 2007. The work is supported in part by the Foundation of Research, Science and Technology (FRST) Grant, New Zealand, under contract number UOAX0406.

References

[1] Anderson K, Throckmorton GS, et al. The effects of bolus hardness on masticatory kinematics. J Oral Rehab 2002;29:689–96.
[2] Foster K, Woda A, Peyron M-A. Effect of texture of plastic and elastic model foods on the parameters of mastication. J Neurophysiol 2006;95:3469–79.
[3] Daumas B, Xu WL, Bronlund J. Jaw mechanism modeling and simulation. Mech Mach Theory 2005;40(7):821–33.
[4] Xu WL, Bronlund J, Kieser J. A robotic model of human masticatory system for reproducing chewing behaviours. IEEE Robot Automat Mag 2005;12(2):90–8.
[5] Takanobu H, Takanishi A, Ozawa D, Ohtsuki K, Ohnishi M, Okino A. Integrated dental robot system for mouth opening and closing training. In: Proceedings of the 2002 IEEE international conference on robotics & automation, Washington, DC; 2002. p. 1428–33.
[6] Takanobu H, Takanishi A. Dental robotics and human model. In: Proceedings of the 1st international IEEE EMBS conference on neural engineering, Capri Island; 2003. p. 671–4.
[7] Xu WL, Pap JS, Bronlund J. Design of a biologically inspired robot for foods chewing. IEEE Trans Ind Electron 2008;55(2):832–41.
[8] Xu WL, Torrance J, Pap J-S, Chen B, Potgieter J, Bronlund J. Kinematics and experiments of a life-sized chewing robot for characterising food texture. IEEE Trans Ind Electron 2008;55(5):2121–32.
[9] Latash ML. Neurophysiological basis of movement, human kinetics. Champaign, IL; 1998. 267p.
[10] Lund JP. Mastication and its control by the brain stem. Critical Rev Oral Biol Med 1991;2(1):33–64.
[11] Turker KS. Reflex control of human jaw muscles. Critical Rev Oral Biol Med 2002;13(1):85–103.
[12] van der Bilt A, Engelen L, et al. Oral physiology and mastication. Physiol Behav 2006;89:22–7.
[13] Gonalez R, Montoya I, Carcel J. Review: the use of electromyography on food texture assessment. Food Sci Tech Int 2001;7(6):461–71.
[14] Peyron MA, Lassauzay C, Woda A. Effects of increased hardness on jaw movement and muscle activity during chewing of visco-elastic model foods. Exp Brain Res 2002;142:41–51.
[15] Ellias S, Grossberg S. Pattern formation, contrast control, and oscillations in the short term memory of shunting on-center off-surround networks. Biol Cybernet 1975;20:69–98.
[16] Matsuoka K. Sustained oscillations generated by mutually inhibiting neurons with adaptation. Biol Cybernet 1985;52:367–73.
[17] Iwasaki T, Zhang M. Sensory feedback mechanism underlying entrainment of central pattern generator to mechanical resonance. Biol Cybernet 2006;94:245–61.
[18] Kotoh R, Mori M. Control method of biped locomotion giving asymptotic stability of trajectory. Automatica 1984;20(4):405–14.
[19] Buchli J, Righetti L, Ijspeert AJ. Engineering entrainment and adaptation in limit cycle systems, from biological inspiration to applications in robotics. Biol Cybernet 2006;95:645–64.
[20] Williamson MM. Robot arm control exploiting natural dynamics, PhD Thesis, Massachusetts Institute of Technology; 1999. 192p.
[21] Berthouze L, Lungarella M. Motor skill acquisition under environmental perturbations: on the necessity of alternate freezing and freeing of degrees of freedom. Adaptive Behav 2004;12(1):47–64.
[22] Matsuoka K. Sustained oscillations generated by mutually inhibiting neurons with adaptation. Biol Cybernet 1987;56:345–53.
[23] Koolstra JH, van Eijden TMGJ. Dynamics of the human masticatory muscles during a jaw open-close movement. J Biomech 1997;30:883–9.
[24] Eijden TMGJ, Korfage JAM, Brugman P. Architecture of the human jaw-closing and jaw-opening muscles. Anatomical Record 1997;248:464–74.
[25] Koolstra JH, van Eijden TMGJ. Combined finite-element and rigid-body analysis of human jaw joint dynamics. J Biomech 2005;38:2437–9.
[26] Low KH, Wang H, Wang MY. On the development of a real time control system by using xPC Target: solution to robotic system control. In: Proceedings of the 2005 IEEE, international conference on automation science and engineering, Canada; 2005, p. 345–50.